Precipitant molar concentration effect on the upconversion emission in BaZrO3:Er,Yb nanocrystalline phosphor

L.A. Diaz-Torres*,[a], P.Salas [b], V.M. Castaño[b], J. Oliva [a], C. Angeles-Chavez[c] .
a Centro de Investigaciones en Optica A.C., Leon, Gto. 37150 Mexico.
b Centro de Física Aplicada y Tecnología Avanzada, Universidad Nacional Autónoma de México, A. P. 1-1010, Querétaro 76000, Mexico.
C [4] Instituto Mexicano del Petróleo, A. P. 14-805, Cd. De México, D.F., 07730 México.

* corresponding author: ditlacio@cio.mx.

ABSTRACT

Strong green and red upconversion emissions of Er3+ in nanocrystalline BaZrO3:Yb,Er is observed. Powder samples were obtained by a facile hydrothermal process at 100°C under different NaOH molar concentrations and annealed in air at 1000°C for 24 h. Band gap and luminescence depend on precipitant molar concentration. Well faceted single phase BaZrO3 secondary particles were obtained for precipitant concentrations of 1.0 M whereas for other precipitant concentrations ZrO2 segregation was observed.

Keywords
Hydrothermal synthesis, barium zirconate, upconversion, Ytterbium, Erbium

1 INTRODUCTION

Upconversion (UPC) is the generation of visible or UV light by excitation with larger wavelengths, usually NIR, of trivalent rare-earth (RE) ions supported into a solid-state host. It is one of the nonlineal processes most widely investigated in the two last decades, as well as the trivalent RE ions in different host matrix in order to generate such optical process [1-3]. Practical UPC phosphors from ultra-violet to green spectral range have a wide range of applications as high-density optical storage, color displays, optical fiber communications, and recently as biological labels for medical imaging [4-6]. UPC of Er3+ doped host sensitized with Yb3+ has been widely studied in matrices such as GGG, NaYF4, ZrO2, LaF3, Y2O3 and YAG [7-11], and recently in BaZrO3 [12]. The excited state of the Yb3+ ion (10,000cm^{-1}) has a broad absorption band between 800 and 1100 nm and a much higher absorption cross-section than the 4I11/2 excited state of Er3+. The large spectral overlap between Yb3+ emission (2F5/2→2F7/2) and Er3+ absorption (4I15/2→4I11/2) results in an efficient resonant energy transfer (ET) from Yb3+ to Er3+ in Yb3+–Er3+-codoped systems. It is well known that in the UPC emission of RE ions, the highest phonon frequencies of the host lattice are responsible for nonradiative relaxation, resulting in a reduction of quantum efficiency. Then, matrices with low phonon energy are much more favorable in promoting the upconversion process. Although Fluorides have the best upconversion conversion efficiencies on account of very low phonon energies, they lack chemical stability. In most cases Fluorides are hydroscopic and that poses a serious drawback for biological applications and luminescent systems subject to humid environments. The oxides, on the contrary, are quite resistant to corrosive environments and have good optical properties. However, most perovskites have temperature phase transformations that lead to anisotropies in their refraction index, and this causes non linear optical phenomena such as second harmonic generation [1]. For some high energy upconversion applications this becomes a limiting factor since the upconversion generated heat can lead to such induced anisotropies limiting the range of pump power. Barium zirconate ($BaZrO_3$) is a very promising refractory structural material with a very high melting point (2600 ºC) and a low chemical reactivity towards corrosive compounds like the ones used in the fabrication of high temperature superconductors. Among the cubic oxide perovskites, $BaZrO_3$ (BZO) is the only one that does not follow phase transitions over the range from 1600 K down to 4 K [13]. Recently, columnar inclusions of BZO nanocrystallites were found to enhance the transport currents in YBCO superconductors [14]. Besides, $BaZrO_3$ has attracted attention as a promising candidate for protonic electrolytes in Fuel cell applications [15]. In this paper, we report on the effects of the NaOH precipitant concentration, in the hydrothermal synthesis, on the morphology and upconversion emission of BZO of nanocrystalline particles. Green and red visible upconversion in Yb3+-Er3+ codoped BZO is explored under 978 nm excitation.

2 EXPERIMENTAL

Yb^{3+}–Er^{3+} codoped BZO microparticles were obtained by a facile hydrothermal process. RE content was fixed to 1 mol % Yb_2O_3 and 1 mol % Er_2O_3. All chemicals were analytical grade from Sigma Aldrich Inc. and were used as

received. Barium nitrate ($Ba(NO_3)_2$), zirconyl chloride octahydrate ($ZrOCl_2$ $8H_2O$), erbium nitrate ($Er(NO_3)_3$ $5H_2O$) and ytterbium nitrate ($Yb(NO_3)_3$ $5H_2O$) were used as the starting materials for the Yb^{3+}–Er^{3+} co-doped BZO samples. Sodium hydroxide (NaOH) was used as the precipitating agent. Cetyl-trimethyl-ammonium-bromide (CTAB) was used as the surfactant. In a typical procedure, barium nitrate (4.53 g), zirconyl chloride (5.58 g), erbium nitrate (0.16 g), ytterbium nitrate (0.32 g) and CTAB (1.9 g) were dissolved in a 1:1 solution of ethanol-water at room temperature applying vigorous stirring for 1 h. Under strong stirring NaOH was added at three different molar concentrations: 0.1 M, 1.0 M, and 2.0 M. The hydrothermal reactions were carried out in a Teflon autoclave (500 ml in total capacity) under autogenous pressure at 100 ºC for 24 h. The precipitate was then washed with distilled water and dried in an oven at 100 ºC for 15 hr, and then annealed at 1000 ºC for 3 h, with a heating rate of 3 ºC/min.

The X-ray diffraction (XRD) patterns of as prepared and annealed samples were obtained using a SIEMENS D-500 equipment provided with a Cu tube with Kα radiation at 1.5405 Å, scanning in the 20º to 70º 2θ range with increments of 0.02º and a sweep time of 1 s. The morphology of the nanocrystalline particles was analyzed by scanning electron microscopy (SEM) using a Hitachi S-4500II operating at 25 kV. For absorption spectra, 7 mm diameter pellets were obtained by pressing the powder samples at 15 Ton pressure. Visible absorption spectra measurements were carried out in a Lambda 900 Perkin Elmer spectrophotometer in the reflectance mode with a 1 inch integrating sphere from Labsphere Co. The photoluminescence characterization was performed under 978 nm excitation form a tunable OPO system (MOPO from Spectra Physics) pumped by the third harmonic of a 10 ns Nd:YAG pulsed laser. The fluorescence emission was analyzed with a Acton Pro 500i spectrograph and a Hamamatsu photomultiplier tube R7400U-20 connected to a SR860 lock-in amplifier (Stanford Research). All photoluminescence measurements were done at room temperature. Special care was taken to maintain the alignment of the set up in order to compare the intensity of the upconversion signal produced by different samples.

3 RESULTS AND DISCUSSIONS

Secondary particles of regular shape and low dispersion in size were obtained for NaOH concentrations of 1 and 2 M, see SEM micrographs a) and b) in figure 1. Whereas for a NaOH concentration of 0.5 M the obtained particles were irregular in shape and with sizes ranging from nanoparticles to a few microns, see SEM micrograph c) in figure 1. These secondary particles are nanocrystalline aggregates of smaller nanoparticles as can be observed in figure 1b, and in figure 1S in supplementary information. The XRD patterns shown in figure 1 for the three NaOH precipitant concentrations suggest a good degree of crystallinity. For all samples the main peaks in the XRD patterns are in agreement with the JCPDS60399 standard for cubic BaZrO3, marked with stars. However for the 0.5 and 2.0M NaOH there are other well resolved peaks that correspond to a monoclinic zirconia phase, marked by arrows in figure 1. This suggests deviations in NaOH precipitant molar concentrations from 1.0 M promote the segregation of zirconia phase. This is in agreement with the fact that pH control is a critical parameter in hydrothermal synthesis. Thus, a concentration of 1 M of NaOH leads to a estequiometric precipitation of Ba and Zr hydroxide precursors which after subsequent thermal treatments result in estequiometric BaZrO3. When the molar concentrations of NaOH are higher than 1 M a faster formation of zirconium oxide precursors leads to its segregation from the BZO phase. The same happens to a greater extent for NaOH molar concentrations lower than 1 M. In fact, for the 0.5 M NaOH concentration, such great non-estequiometric balance in Zr and Ba hydroxide precursors inhibits the aggregation of the well faceted secondary particles observed for 1.0 and 2.0 M NaOH. This might be due to the excess of ZrO2 nanoparticles which form faster than the BaZrO2 nanoparticles, and then during the annealing process the excess of ZrO2 nanoparticles inhibits the coalescence of the BaZrO3 nanoparticles.

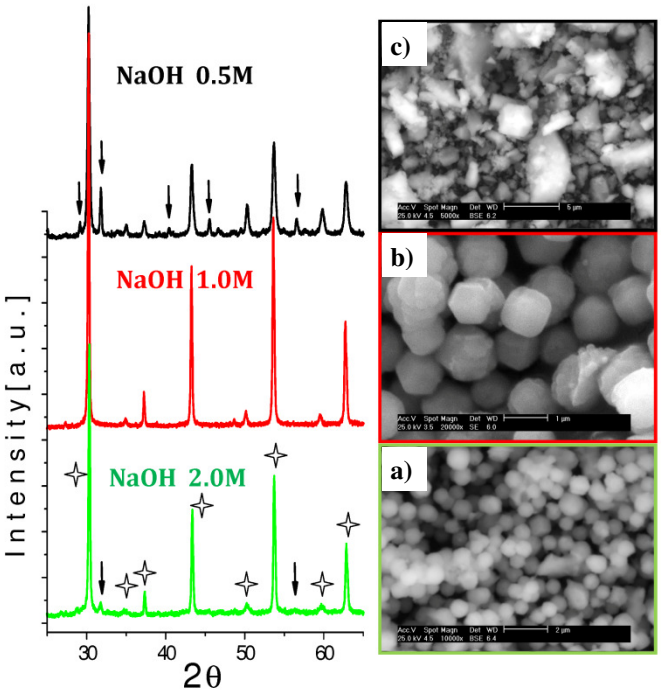

Figure 1. XRD patterns of BaZrO3 samples for different NaOH molar concentrations, and annealed at 1000°C. Bars in micrographs correspond to a) 5 µm, b) 1 µm, and c) 2 µm. as synthesized. Arrows correspond to main peaks of monoclinic zirconia. Stars correspond to the mail peaks of the JCPDS60399 standard for cubic BaZrO3.

Room Temperature (RT) absorption spectra for the three BZO samples annealed at 1000 ºC are shown in figure 2. All bands in the spectra have been identified and

correspond to the transitions from the ground state of Er (or Yb) ions to the final state of Er (or Yb) ions as indicated in figure 2. As expected, the main difference between these spectra is in the range between 800 to 1000 nm where Yb ions have its well known absorption band, of its only exited state $^4F_{5/2}$, superimposed on the $^4I_{11/2}$ absorption of the Er ions. The broad band centered at 1482 nm, that is superimposed with the absorption band of the 4I13/2 Er state, indicates the presence of residual OH anions that haves been kept occluded within the BZO crystallites. One might note that such band is quite strong in the sample with smaller NaOH molar concentration, which is also the one with an irregular morphology and a high particle size dispersion. Bandgap estimations, from the absorbance spectra in Kubelka-Munk units [16] has depicted in the inset of figure 2, were in the range between 3.75 and 4.57 eV in agreement with the reported values for BZO [17]. It is observed that the band gap decreases as NaOH molar concentration decreases. The band gap for the lower NaOH concentration is smaller than the expected value of 4.8 eV for well ordered bulk BZO [17], that suggest that this sample has a lot of defects, might be due to the high segregation of zirconia nanoparticles. The other two samples have bandgap values closer to the bulk value, and their lower bandgap are assumed to be a consequence of its nanocrystalline nature.

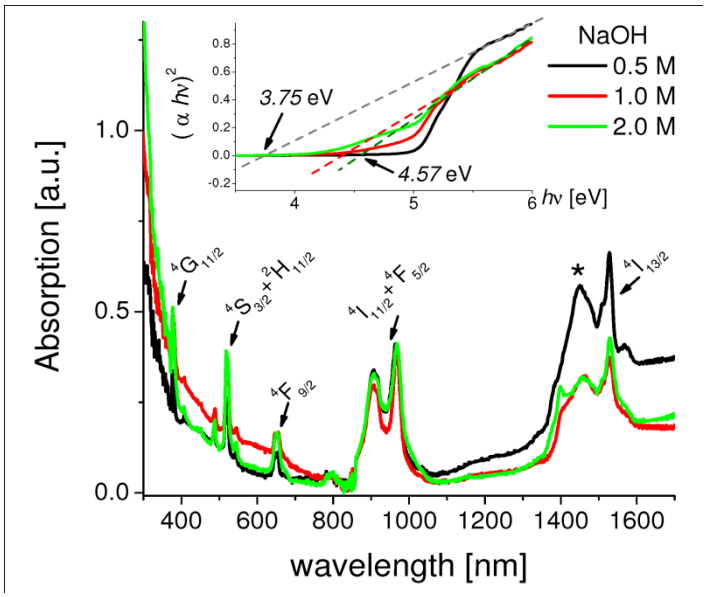

Figure 2. Absorption spectra of the three BZO samples annealed at 1000°C. Inset shows the absorbance Kubelka-Munk units.

Under NIR excitation at 978 nm upconverted Er3+ emissions in the green ($^2H_{11/2} + {}^4S_{3/2} \rightarrow {}^4I_{15/2}$) and red ($^4F_{9/2} \rightarrow {}^4I_{15/2}$) regions are observed for all synthesized samples, see figure 3. Both upconversion emission have similar structures, but different red to green intensity ratios. The higher red to green ratio corresponds to the 0.5 M NaOH sample which is the one with the greater segregation of zirconia nanoparticles. The following red to green ratio corresponds to the 2.0 M NaOH that has less zirconia segregation than the 0.5 M NaOH sample, and the smaller red to green ratio corresponds to the 1.0 M NaOH sample that has no measurable zirconia segregation. This is in agreement with previous reports that reduction on nanocrystals size in Er-Yb codoped phosphors leads to an increasing red to green ratio [2,4,7]. This suggests that as NaOH concentration increases in our BZO samples the nanocrystalline secondary particles have smaller sizes, and that as NaOH concentrations reduces from 1.0 M the amount of zirconia nanocrystals increases as well.

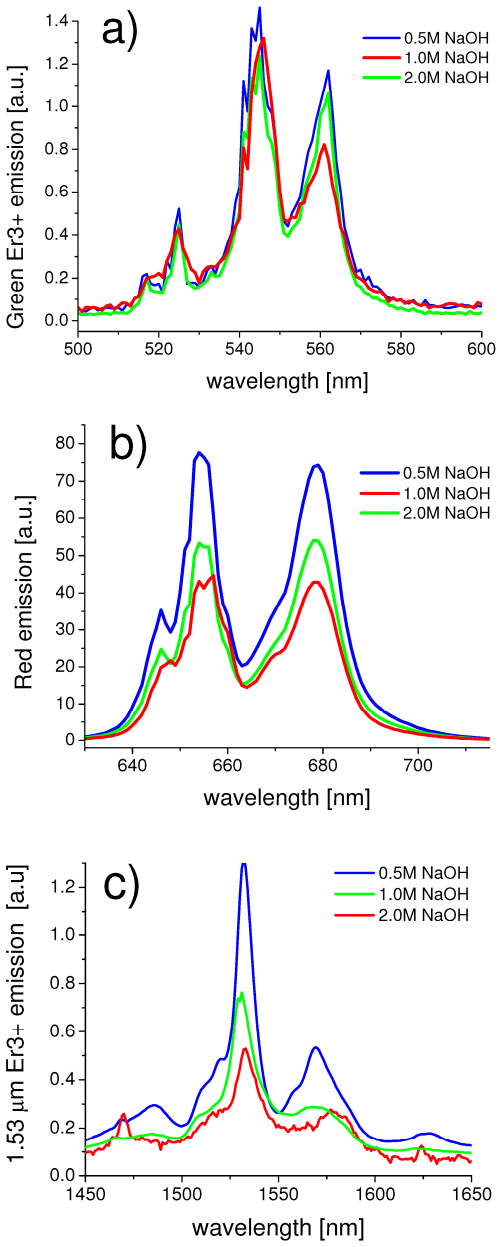

Figure 3. Emissions of Er3+ ions under 978 nm. a) and b) correspond to the Er3+ green and red upconversion emissions, respectively; and c) corresponds to the 1.53 mm emission from Er3+ ions.

Near infrared emission at 1.53μm from the ($^2I_{13/2} \rightarrow {}^4I_{15/2}$) transition of Er3+ ions is also observed for all samples, see figure 3c. It is observed that for the samples with zirconia segregation as NaOH molar concentration increases the 1.53μm emission decreases, in agreement with the fact that the overall amount of zirconia phase is decreasing. In addition the 1.53μm emission from the 1.0 M NaOH concentration is the weaker one since it has almost no zirconia content. The fact that the 1.53μm band structure for this latter sample is quite different from the band structure of the two former samples suggest that the Er3+ ions have been substituted in the Zr4+ sites within the BZO cubic phase. Besides, the lower level of emission supports the fact that the Er3+ ions are substituted in sites of lower symmetry [7]. In summary, segregation of zirconia might affect considerably the red and NIR emissions of BZO nanocrystalline particles, and such segregation strongly depends on the molar concentration of the precipitant used in the hydrothermal synthesis.

4 CONCLUSIONS

In summary, we have obtained BZO nanocrystalline secondary well faceted particles. Morphologies and phase composition as well as upconversion and NIR emissions depend strongly on the molar concentration of the precipitant used in the hydrothermal synthesis. Thus there is a compromise between morphology and phase versus overall emission intensities, both in the visible and near infrared regions. The best morphology corresponds to a NaOH molar concentration of 1.0 M, whereas the best emission properties correspond to a 0.5 M concentration of NaOH.

5 REFERENCES

[1] Boulon, G., Journal of Alloys and Compounds 451 (2008) 1–11.

[2] Chen, G. et al., *Nanotechnology* 20 (38), art. no. 385704.

[3] Auzel, F., *Chemical Reviews* 104 (1), pp. 139-173.

[4] Chen, G., et al., Phys. Rev. B 75, art. No. 195204.

[5] Jiang, C. et al., *Nanotechnology* 20 (15), art. no. 155101.

[6] Xu, C.T. et al., *Applied Physics Letters* 93 (17), art. no. 171103.

[7] Vetrone, F. et al., *Journal of Physical Chemistry B* 107 (39), pp. 10747-10752.

[8] Zhang, Q. et al, *Journal of Colloid and Interface Science* 336 (1), pp. 171-175.

[9] Salas, P. et al, *Optical Materials* 27 (7), pp. 1295-1300.

[10] Qu, Y. et al., *Materials Letters* 63 (15), pp. 1285-1288.

[11] Martinez A. et al., *Microelectronics Journal* 39 (3-4), pp. 551-555.

[12] Hinojosa, S. et al., *Optical Materials* 27 (12), pp. 1839-1844.

[13] P.G. Sundell, M.E. Björketun, G. Wahnström, Phys Rev B 73, 104112 (2006).

[14] S. Kang, A. Goyal, J. Li, A.A. Gapud, P.M. Martin, L. Heatherly, J.R. Thompson, D.K. Christen, F.A. List, M. Paranthaman, DF Lee, Science 311(31), 1911 (2006).

[15] A. S. Patnaik, A.V. Virka, J Electrochem Soc, 153(7), A1397 (2006).

[16] P. Kubelka and F. Munk, Z. Tech. Phys. (Leipzig) 12, (1931) 593.

[17] Cavalcante, L. S.; Longo, V. M.; Zampieri, M.; Espinosa, J. W. M.; Pizani, P. S.; Sambrano, J. R.; Varela, J. A.; Longo, E.; Simones, M. L.; Paskocimas, C. A. J. Appl. Phy. 103, (2008) art No. 063527.

[18]

[19]